Bulletin of Mathematical Biology (2008) 70: 253–280
DOI 10.1007/s11538-007-9255-4

ORIGINAL ARTICLE

Circulating Vaccine Derived Polio Viruses and their Impact on Global Polio Eradication

Bradley G. Wagner*, David J.D. Earn

Department of Mathematics and Statistics, McMaster University, 1280 Main Street West, Hamilton, ON L8S 4K1, Canada

Received: 22 November 2006 / Accepted: 22 June 2007 / Published online: 13 October 2007

Abstract Poliomyelitis vaccination via live Oral Polio Vaccine (OPV) suffers from the inherent problem of reversion: the vaccine may, upon replication in the human gut, mutate back to virulence and transmissibility resulting in circulating vaccine derived polio viruses (cVDPVs). We formulate a general mathematical model to assess the impact of cVDPVs on prospects for polio eradication. We find that for OPV coverage levels below a certain threshold, cVDPVs have a small impact in comparison to the expected endemic level of the disease in the absence of reversion. Above this threshold, the model predicts a small but significant endemic level of the disease, even where standard models predict eradication. In light of this, we consider and analyze three alternative eradication strategies involving a transition from continuous OPV vaccination to either continuous Inactivated Polio Vaccine (IPV), pulsed OPV vaccination, or a one-time IPV pulse vaccination. Stochastic modeling shows continuous IPV vaccination is effective at achieving eradication for moderate coverage levels, while pulsed OPV is effective if higher coverage levels are maintained. The one-time pulse IPV method may also be a viable strategy, especially in terms of the number of vaccinations required and time to eradication, provided that a sufficiently large pulse is practically feasible. More investigation is needed regarding the frequency of revertant virus infection resulting directly from vaccination, the ability of IPV to induce gut immunity, and the potential role of spatial transmission dynamics in eradication efforts.

Keywords Oral polio vaccine (OPV) · Vaccine reversion · Vaccine associated paralytic polio (VAPP) · Epidemiology · Mathematical modeling

*Corresponding author.
E-mail addresses: wagnerb@math.mcmaster.ca (Bradley G. Wagner), earn@math.mcmaster.ca (David J.D. Earn).
B.G. Wagner's research is supported by the Natural Sciences and Engineering Research Council of Canada (NSERC) Doctoral Scholarship.
D.J.D. Earn's research is supported by the Canadian Institutes of Health Research (CIHR), Natural Sciences and Engineering Research Council of Canada (NSERC) and the J.S. McDonnell Foundation.

1. Introduction

Vaccination for a number of diseases is currently performed through administration of live-attenuated virus vaccines. Attenuation means that the virus has been altered genetically into a state of low virulence and low transmissibility. Attenuation is often accomplished by passage through successive animal host tissues in which there is selective pressure for mutations that reduce the virulence and transmissibility in humans; this differs from inactivated virus vaccines where the virus is killed by treatment with a chemical agent or some physical process (Woodrow and Levine, 1990). An intrinsic problem with live-attenuated virus vaccines is that of back mutation or reversion, whereby the live virus, upon replicating in its human host, may regain its virulence and transmissibility, potentially causing infection in the vaccinee and his or her contacts. Reversion to higher transmissibility is a potentially serious barrier to disease eradication.

An important and well documented example in which reversion takes place is in the use of Oral Polio Vaccine (OPV). Poliovirus is an RNA virus, and may appear in one of three antigenic types. Transmission may be either fecal to oral, or oral to oral. Initially, the virus resides in the pharynx and intestines of the host. Subsequently, it may invade the local lymphoid tissue, entering the blood stream and eventually invading the motor neurons. Damage to these neurons may result in varying degrees of paralysis. It should be noted that there is no cross immunity between antigenic types. As well, the standard formulation of OPV is *trivalent*: it contains attenuated versions of all three types (each of which is capable of undergoing reversion and potentially causing paralysis (Anon, 1994)).

In cases where OPV vaccination results in paralysis, this effect is commonly referred to as vaccine associated paralytic polio (VAPP). Vaccine viruses which have regained transmissibility and neurovirulence are referred to as circulating vaccine derived polioviruses (cVDPVs) (John, 2004).

Though largely replaced in the developed world by the Salk injectable inactivated polio virus vaccine (IPV) (Anon, 2005a), OPV is still the primary vaccine in the developing world. Since 1988, the World Health Organization (WHO) has advocated the exclusive use of OPV for polio eradication, citing five primary factors: (1) low cost, (2) simple administration (oral), (3) high effectiveness for a small number of doses, (4) ability to induce a high level of intestinal immunity, and (5) the possibility of contact vaccination whereby vaccinated individuals may spread the vaccine virus resulting in secondary immunizations (John, 2004).

While the efficacy of OPV is generally excellent, it has been shown to induce a reduced immune response in some individuals living in regions where diarrheal disease is highly endemic. Recent work has traced the problem to the use of trivalent OPV. Studies now show that monovalent OPV can be used to achieve a high level of efficacy in the regions where standard trivalent OPV has been problematic (Grassly et al., 2007). Consequently, vaccine efficacy should not presently represent a concern for OPV.

The drawbacks of OPV are the risk of VAPP and the creation of cVDPVs. IPV, on the other hand, involves no risk of reversion as it is a killed virus. However, IPV has the disadvantages that it is roughly five times more expensive to produce (Offit, 2005), must be injected, cannot produce contact vaccinations, and is believed to induce a lower level of intestinal immunity (Laasri et al., 2005). Intestinal immunity is important as vaccinated individuals with no intestinal immunity can still have polio virus replicating in their intestines, and thus serve as carriers of the disease (in spite of being immune themselves).

Recent studies show enhanced potency IPV (eIPV) provides improved intestinal immunity, but eIPV is still believed to be inferior to OPV in this respect (Laasri et al., 2005).

The creation of cVDPVs from OPV poses an obstacle to eventual polio eradication. Since 2000, four outbreaks of cVDPVs have been identified in Madagascar, the Philippines, Hispaniola and China (Heymann et al., 2005). In the cases of China and Hispaniola, these outbreaks occurred more than 5 years after the regions had been certified as polio free. It is important to note that detection of cVDPVs is complicated by the fact that most polio infections cause little or no illness: the ratio of paralytic to inapparent or asymptomatic polio has been estimated to be 1:200 (Heymann et al., 2005; Anon, 2005a).

In this work, we investigate an infectious disease transmission model that includes the possibility of reversion. We provide tools to assess the epidemiological impact of reversion, and the creation of cVDPVs, assuming the present polio vaccination strategy in developing countries (continuous OPV vaccination). We then address the problem of polio eradication, presenting three alternative polio eradication strategies involving both IPV and OPV and comparing their effectiveness. The mathematical model is built from the basic SIR model, which we review first. Although we focus on polio here, we emphasize that the model is relevant to many diseases for which live virus vaccines exist.

2. The basic SIR model

The basic Susceptible-Infected-Removed (SIR) model is the simplest transmission model for diseases that confer lifelong immunity. In spite of its simplicity, it successfully predicts the shape of epidemic curves (Kermack and McKendrick, 1927) and yields useful quantitative predictions of eradication thresholds (Anderson and May, 1991).

We will assume initially that the population is sufficiently large that we can treat the number of individuals who are susceptible ($\tilde{S}$), infected ($\tilde{I}$) or removed ($\tilde{R}$) as continuous variables. Note that "infected" individuals are assumed to be infectious and "removed" individuals are immune to the pathogen. If a vaccine exists and a fixed proportion of individuals is vaccinated as soon as any maternally-acquired immunity has waned, the model can be written

$$\frac{d\tilde{S}}{dt} = (1-p)\nu N - \frac{\beta}{N}\tilde{I}\tilde{S} - \mu\tilde{S}, \tag{1a}$$

$$\frac{d\tilde{I}}{dt} = \frac{\beta}{N}\tilde{I}\tilde{S} - (\mu+\gamma)\tilde{I}, \tag{1b}$$

$$\frac{d\tilde{R}}{dt} = p\nu N + \gamma\tilde{I} - \mu\tilde{R}. \tag{1c}$$

Here, the total population is $N = \tilde{S} + \tilde{I} + \tilde{R}$. The parameters of the model are the proportion vaccinated (p), the birth rate (ν, for *natality*), the transmission rate (β), the recovery rate (γ) and the natural death rate (μ, for *mortality*). The mean infectious period is $1/\gamma$. The model assumes that immunity is lifelong and that there is no disease-induced mortality (or that disease-induced mortality is sufficiently rare that its dynamical effect is negligible). It should also be noted that individuals may be asymptomatic for part (or all) of the infectious period.

Equation (1) is forward invariant in the non-negative orthant $\{(\tilde{S}, \tilde{I}, \tilde{R}) \mid \tilde{S} \geq 0, \tilde{I} \geq 0, \tilde{R} \geq 0\}$, so initially non-negative solutions can never become negative. To see this, note that if $\tilde{S} = 0$ then $d\tilde{S}/dt \geq 0$ (and similarly for $\tilde{I}$ and $\tilde{R}$).

It is more convenient to work with the SIR model in terms of proportions of the population, so we apply the variable transformations

$$S = \frac{\tilde{S}}{N}, \qquad I = \frac{\tilde{I}}{N}, \qquad R = \frac{\tilde{R}}{N}. \tag{2}$$

If the population is constant (i.e., $\nu = \mu$, which is an excellent approximation when looking at short time scales) then Eq. (2) simply represents scaling by a constant. More generally, N will grow (or decay) at exponential rate $\nu - \mu$. Noting that

$$\frac{d\tilde{X}}{dt} = \frac{1}{N}\frac{dX}{dt} - \frac{X}{N^2}\frac{dN}{dt}, \tag{3}$$

where X is S, I or R, we obtain the SIR model in terms of proportions:

$$\frac{dS}{dt} = (1-p)\nu - \beta I S - \nu S, \tag{4a}$$

$$\frac{dI}{dt} = \beta I S - \gamma I - \nu I, \tag{4b}$$

$$\frac{dR}{dt} = p\nu + \gamma I - \nu R. \tag{4c}$$

The forward invariance of Eq. (1) in the non-negative orthant implies that Eq. (4) is forward invariant in the simplex $\{(S, I) \mid 0 \leq S \leq 1, 0 \leq I \leq 1, 0 \leq S + I \leq 1\}$. Furthermore, as $S + I + R = 1$, one of these equations is redundant, so we drop Eq. (4c).

In subsequent sections, we will employ Eq. (4) to model continuous IPV vaccination, as reversion is not an issue for the killed virus vaccine.

2.1. Analysis of the basic SIR model

A key characteristic of an infectious disease in a given population is its basic reproductive ratio, $\mathcal{R}_0$, which is defined to be the average number of secondary infections caused by a single infected individual in a population with no immunity. $\mathcal{R}_0$ is the product of the transmission rate and the mean time that an individual is infectious, hence for the model given by Eq. (4) (with constant population)

$$\mathcal{R}_0 = \frac{\beta}{\gamma + \nu}. \tag{5}$$

System (4) has two equilibria. Denoting the equilibrium proportions of individuals that are susceptible and infected by S^* and I^*, respectively, the *disease free equilibrium* (DFE) is

$$S_1^* = 1 - p, \qquad I_1^* = 0. \tag{6}$$

The *endemic equilibrium* is

$$S_2^* = \frac{1}{\mathcal{R}_0}, \qquad I_2^* = \frac{\nu}{\gamma + \nu}\left(1 - \frac{1}{\mathcal{R}_0} - p\right). \tag{7}$$

It is convenient to define two further dimensionless quantities in terms of the model parameters:

$$f = \frac{\nu}{\gamma + \nu}, \tag{8}$$

which is the mean time spent in the infected class as a fraction of mean life-span (assuming a constant population) and

$$p_{\text{crit}} = 1 - \frac{1}{\mathcal{R}_0}. \tag{9}$$

We can then express the endemic equilibrium as

$$S_2^* = \frac{1}{\mathcal{R}_0}, \qquad I_2^* = f(p_{\text{crit}} - p), \tag{10}$$

from which we see that p_{crit} is the *critical vaccination level*: the endemic equilibrium exists (i.e., is positive and hence biologically meaningful) if and only if $p < p_{\text{crit}}$. It can be shown that if the vaccination proportion $p \geq p_{\text{crit}}$ then the DFE is globally asymptotically stable (states near the DFE stay near the DFE and every solution eventually approaches the DFE). Similarly, if $p < p_{\text{crit}}$ then any initial condition with $I(0) > 0$ eventually converges to the endemic equilibrium (Hethcote, 2000; Korobeinikov and Wake, 2002). Biologically, p_{crit} is an eradication threshold: the disease will persist if and only if $p < p_{\text{crit}}$. Note that this critical vaccination proportion is determined solely by the basic reproductive ratio $\mathcal{R}_0$. The proportion of the population that is immune at a given time is often called the degree of *herd immunity*. Thus, p_{crit} is the level of herd immunity that must be maintained to prevent persistence should an eradicated disease be reintroduced.

3. The live-attenuated vaccine model: modeling OPV

To account for the effects of a live-attenuated virus vaccine such as OPV, we assume a fixed proportion of those vaccinated will become infected by the revertant virus. All other vaccinations are taken to be successful at conferring immunity without illness. Leaving the other aspects of the SIR model intact, the new model can be depicted graphically as in Fig. 1 and expressed mathematically (in terms of *proportions* S, I and R) via

$$\frac{dS}{dt} = (1-p)\nu - \beta IS - \nu S, \tag{11a}$$

$$\frac{dI}{dt} = \phi p\nu + \beta IS - \gamma I - \nu I, \tag{11b}$$

$$\frac{dR}{dt} = (1-\phi)p\nu + \gamma I - \nu R. \tag{11c}$$

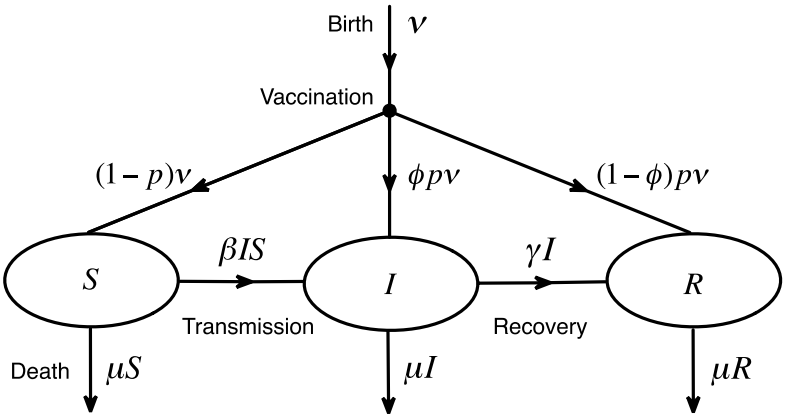

Fig. 1 Flow diagram for the live-attenuated vaccine model that we use to investigate the effects of OPV on polio transmission. The flow diagram for the basic SIR model (Eq. (1)) is obtained by setting the reversion factor ϕ to zero. The model (for any value of ϕ) is expressed in Eq. (11) in terms of *proportions* of the population that are susceptible, infectious or removed.

Here ϕ is the *reversion factor*, i.e., the proportion of those vaccinated who become infected by the revertant virus ($0 < \phi \leq 1$). As in Eq. (4), Eq. (11c) is superfluous and we deal with the two-dimensional system defined by Eqs. (11a) and (11b). Note that since the three types of polio do not interact immunologically, we have not included any strain structure in the model.

There has been considerable recent interest in models that include a separate compartment for vaccinated individuals (Brauer, 2003), rather than simply the proportion vaccinated as specified by p in Eq. (11). A separate vaccinated compartment can be important if the vaccine has limited efficacy (or if vaccine-induced immunity wanes) because vaccinated individuals may remain (or become) partially susceptible. The "breakthrough infections" that occur in this situation typically lead to multiple endemic equilibria and backward bifurcations (Brauer, 2003). However, as mentioned in the introduction, OPV is highly efficacious and yields lifelong immunity, so we have not included a separate vaccinated compartment. Our reversion model formalizes the effect of immediate infection that results occasionally from vaccination, as opposed to susceptibility to infection from subsequent exposures following vaccination.

3.1. Epidemiological parameters for poliomyelitis

Epidemiological parameter estimates for poliomyelitis and OPV are given in Table 1. The vaccine reversion factor (ϕ) is estimated indirectly from two parameters that have been estimated previously: the mean number of paralytic polio cases as a proportion of total polio cases (π_{para}) and the incidence of paralytic polio in newly vaccinated infants (V_{infant}). Assuming that VAPP in infants really does result directly from vaccination (as opposed to contact with an infected individual) and that any increase in π_{para} with age can be ignored, the reversion proportion for OPV is

$$\phi = \frac{V_{\text{infant}}}{\pi_{\text{para}}} \approx 10^{-4}. \tag{12}$$

Table 1 Epidemiological parameter estimates for poliomyelitis

Parameter	Symbol	Estimate	Source
Basic Reproductive Ratio	$\mathcal{R}_0$	6	Anderson and May (1991)
Mean Infectious Period	$1/\gamma$	16 days	Anderson and May (1991)
Birth Rate, developed countries	ν	0.02 year^{-1}	McDevitt (1999), Anon (2001)
Birth Rate, developing countries	ν	0.04 year^{-1}	Anon (2001)
$\frac{\nu}{\gamma+\nu}$, developed countries	f	8.76×10^{-4}	Eq. (8) (Section 2.1)
$\frac{\nu}{\gamma+\nu}$, developing countries	f	1.75×10^{-3}	Eq. (8) (Section 2.1)
Infant VAPP Incidence	V_{infant}	1/1400000	Anon (2005a)
Paralytic Polio/Total Polio Cases	π_{para}	1/200	Anon (1994, 2005a)
OPV Reversion proportion	ϕ	10^{-4}	Eq. (12) (Section 3.1)

Note that since OPV contains attenuated versions of all three antigenic types, any of which may revert, we may treat ϕ as an upper bound for reversion in each type.

4. Analysis of the OPV model

4.1. Equilibria

Unlike typical epidemiological models, the OPV model (11) has no DFE. Instead, for any parameter set with $\phi > 0$, there is a single (endemic) equilibrium. Indeed, setting the derivatives to zero in Eqs. (11a) and (11b) and summing the resulting two equations yields

$$S^* = 1 - p(1-\phi) - \frac{1}{f} I^*, \tag{13}$$

where S^* and I^* denote equilibrium values. Inserting (13) into (11b) (set to zero) then yields

$$\frac{1}{f} I^{*2} - \big(p_{\text{crit}} - p(1-\phi)\big) I^* - \frac{p\phi f}{\mathcal{R}_0} = 0. \tag{14}$$

Solving this quadratic for I^* (and insisting that it be non-negative) yields the unique solution

$$I^* = \frac{1}{2} f \big(p_{\text{crit}} - p(1-\phi)\big) + \sqrt{\left[\frac{1}{2} f \big(p_{\text{crit}} - p(1-\phi)\big)\right]^2 + \frac{p\phi f^2}{\mathcal{R}_0}}. \tag{15}$$

Note that $p_{\text{true}} = p(1-\phi)$ is the *true vaccination proportion*, i.e., the proportion of vaccinations that are successful. It is convenient to define

$$\Delta p = p_{\text{crit}} - p(1-\phi). \tag{16}$$

The equilibrium defined by Eqs. (13) and (15) may then be more simply expressed as

$$S^* = 1 - p(1-\phi) - \frac{1}{2}\Delta p - \sqrt{\left[\frac{1}{2}\Delta p\right]^2 + \frac{p\phi}{\mathcal{R}_0}}, \tag{17a}$$

$$I^* = f\left[\frac{1}{2}\Delta p + \sqrt{\left[\frac{1}{2}\Delta p\right]^2 + \frac{p\phi}{\mathcal{R}_0}}\right]. \tag{17b}$$

This equilibrium is always biologically meaningful: it can be shown that (S^*, I^*) lies in the region $\{(S, I) : S > 0, I > 0, S + I < 1\}$ if $0 < p < 1$ and $0 < \phi \leq 1$ (see Appendix A).

4.2. Stability

In this section, we show that the equilibrium (17) is globally asymptotically stable. Biologically, this means that regardless of the proportions of the population that are susceptible (S), infectious (I) and immune (R), the model predicts the virus will persist and approach the endemic prevalence level given by (17b).

We begin by considering how the system behaves if it is perturbed slightly away from the equilibrium. We show that the equilibrium (S^*, I^*) is not only locally stable but always hyperbolic, i.e., that the Jacobian matrix of the system at (S^*, I^*) never has eigenvalues with zero real parts. Hyperbolic stability implies that for any initial conditions sufficiently close to the equilibrium, the solution trajectory converges exponentially to the equilibrium.

4.2.1. Local stability

Linearizing Eqs. (11a) and (11b) about the equilibrium (17) and computing the Jacobian matrix we find

$$J = \begin{pmatrix} -\beta I^* - \nu & -\beta S^* \\ \beta I^* & \beta S^* - (\gamma + \nu) \end{pmatrix}. \tag{18}$$

If $\phi = 0$, the system (11) reduces to the standard SIR model (4) and the equilibrium given by Eqs. (17) corresponds to either the endemic equilibrium (6) of the standard SIR model (for $p < p_{\text{crit}}$) or the DFE (10) of the standard SIR model (for $p \geq p_{\text{crit}}$). In either case, the equilibrium in question is locally asymptotically stable and, provided $p \neq p_{\text{crit}}$, it is hyperbolic (Hethcote, 2000) (J has no eigenvalues on the imaginary axis). If $p = p_{\text{crit}}$ then the DFE of the standard SIR model ($\phi = 0$) is locally asymptotically stable but non-hyperbolic.

The eigenvalues of J can be written

$$\lambda_\pm = \frac{\gamma + \nu}{2}\left\{-(1 + f) + \mathcal{R}_0(S^* - I^*) \right.$$
$$\left. \pm \sqrt{\left[\mathcal{R}_0(S^* + I^*) - (1 - f)\right]^2 - 4\mathcal{R}_0^2 S^* I^*}\right\}. \tag{19}$$

Note that the dependence of these eigenvalues on ϕ is hidden in the expressions for S^* and I^* (Eq. (17)). Since $\lambda_\pm$ depend continuously on ϕ, to prove hyperbolic stability of the equilibrium (17) for any $\phi > 0$ and $p \neq p_{\text{crit}}$ it suffices to show that no eigenvalue of J crosses the imaginary axis as ϕ is varied, for an arbitrary fixed $p \neq p_{\text{crit}}$. Given this, and the fact that the eigenvalues of J are also continuous functions of p, it will follow that the equilibrium is hyperbolically stable also for $p = p_{\text{crit}}$ if we can show that J cannot have an eigenvalue with zero real part for any $\phi > 0$.

Eigenvalues may cross the imaginary axis either at 0 or at Ai where $A \neq 0$. We treat these cases separately. Suppose first that 0 is an eigenvalue of J. Then the determinant of J must be zero, i.e.,

$$\beta I^*(\nu + \gamma) - \nu\beta S^* + \nu(\nu + \gamma) = 0. \tag{20}$$

Using Eq. (13) to write S^* in terms of I^*, and after some algebraic manipulation, we find

$$\frac{2}{f} I^* = \Delta p. \tag{21}$$

Inserting (17b) for I^* into (21) yields

$$\sqrt{\left(\frac{1}{2} f \Delta p\right)^2 + \frac{p\phi f^2}{\mathcal{R}_0}} = 0. \tag{22}$$

But this is impossible for $\phi > 0$, so J does not have a zero eigenvalue.

Now suppose that J has a purely imaginary eigenvalue Ai. Then

$$\det(J - Ai\mathbb{I}) = (-\beta I^* - \nu - Ai)\big(\beta S^* - (\nu + \gamma) - Ai\big) = 0, \tag{23}$$

where $\mathbb{I}$ is the 2×2 identity matrix. Examining the imaginary part of Eq. (23) and simplifying yields

$$-I^* - \frac{\nu}{\beta} + S^* - \frac{1}{\mathcal{R}_0} = 0. \tag{24}$$

Using (13) to express S^* in terms of I^* and rearranging yields

$$\left(1 + \frac{1}{f}\right) I^* + \frac{\nu}{\beta} = p_{\text{crit}} - p_{\text{true}}. \tag{25}$$

As $I^* > 0$, the left-hand side of (25) is strictly positive. Thus if $p_{\text{crit}} \leq p_{\text{true}}$ we have a contradiction. If $p_{\text{crit}} > p_{\text{true}}$ then from Eq. (17b) it is apparent that if $\phi > 0$ then $I^* > f\Delta p = f(p_{\text{crit}} - p_{\text{true}})$. Substituting this inequality into Eq. (25) gives a left-hand side that is strictly greater than $p_{\text{crit}} - p_{\text{true}}$, and we have a contradiction.

Thus, the eigenvalues of J do not cross the imaginary axis for any $\phi > 0$, and the endemic equilibrium given by Eq. (17) is hyperbolically, and hence locally asymptotically stable.

4.2.2. Global stability

As the system is two-dimensional, global asymptotic stability can be established by applying Poincaré–Bendixson theory and Dulac's Criterion (Perko, 1996). Consider an autonomous system of ordinary differential equations,

$$\frac{dx}{dt} = f(x, y), \tag{26a}$$

$$\frac{dy}{dt} = g(x, y), \tag{26b}$$

where f and g are continuously differentiable, and suppose that D is a bounded region in the plane such that there exists a single stable equilibrium point of (26) in the closure of D. If a given orbit remains in D for all $t > 0$ then the Poincaré–Bendixson theorem says that the orbit must either have a non-trivial periodic orbit as its ω-limit set or tend asymptotically to the equilibrium.

Dulac's Criterion states that given a simply connected region D in the plane, with f and g continuously differentiable as above, if there exists a continuously differentiable function $C(x, y)$, such that the divergence of the vector field $\partial_x(Cf) + \partial_y(Cg)$, is not identically zero and does not change sign in D, then there can be no non-trivial periodic orbits contained in D.

Our live-attenuated virus model is a two-dimensional system with orbits bounded (in forward time) in the closure of the triangular region whose boundary is formed by the lines $S \equiv 0$, $I \equiv 0$ and $S + I = 1$ (as discussed for the basic SIR model in Section 2). In fact, we have the stronger condition that the interior of this set, which we denote as $\mathcal{B} = \{(S, I) \mid S > 0, I > 0, S + I < 1\}$, is forward invariant and for all initial conditions on its boundary the flow is into $\mathcal{B}$ (see Appendix C). There is one (hyperbolically) stable equilibrium point in the closure of $\mathcal{B}$, located in $\mathcal{B}$ itself (see Appendix A), and given by Eq. (17). The functions $f(S, I)$ and $g(S, I)$ given by (11a) and (11b) are infinitely differentiable with respect to both S and I. Therefore, applying the Poincaré–Bendixson theory, any orbit must be periodic, have another non-trivial periodic orbit as its ω-limit set, or tend asymptotically to the equilibrium (17). To establish that every orbit must in fact tend to the equilibrium, we rule out the existence of periodic orbits in the closure of $\mathcal{B}$ using the Dulac function

$$C(S, I) = \frac{1}{I}. \tag{27}$$

Notice that $C(S, I)$ is infinitely differentiable in $\mathcal{B}$. Therefore, applying Dulac's criterion yields

$$\partial_S\left(C(S, I)\frac{dS}{dt}\right) + \partial_I\left(C(S, I)\frac{dI}{dt}\right) = -\frac{(I^2\beta + \nu I + p\phi\nu)}{I^2}. \tag{28}$$

Equation (28) is strictly negative for all points in $\mathcal{B}$. Hence, no periodic orbits can exist and by the Poincaré–Bendixson theorem, all orbits must converge to the (hyperbolically) stable equilibrium (17).

4.2.3. Damping frequencies and rate of convergence for polio

4.2.3.1. Damping frequencies Figure 2 shows the frequency of damped oscillations onto the equilibrium (17) as a function of the vaccination proportion p. The birth rate used is representative of developed countries (Table 1). The dashed curve shows the results in the case of zero reversion ($\phi = 0$), corresponding to the standard SIR model, while the solid curve shows results for the estimated OPV reversion proportion ($\phi = 10^{-4}$, Table 1). The damping frequency F_{damp} is given by

$$F_{\text{damp}} = \left|\Im\left(\frac{\lambda}{2\pi}\right)\right|, \tag{29}$$

where λ is either of the two eigenvalues given in Eq. (19).

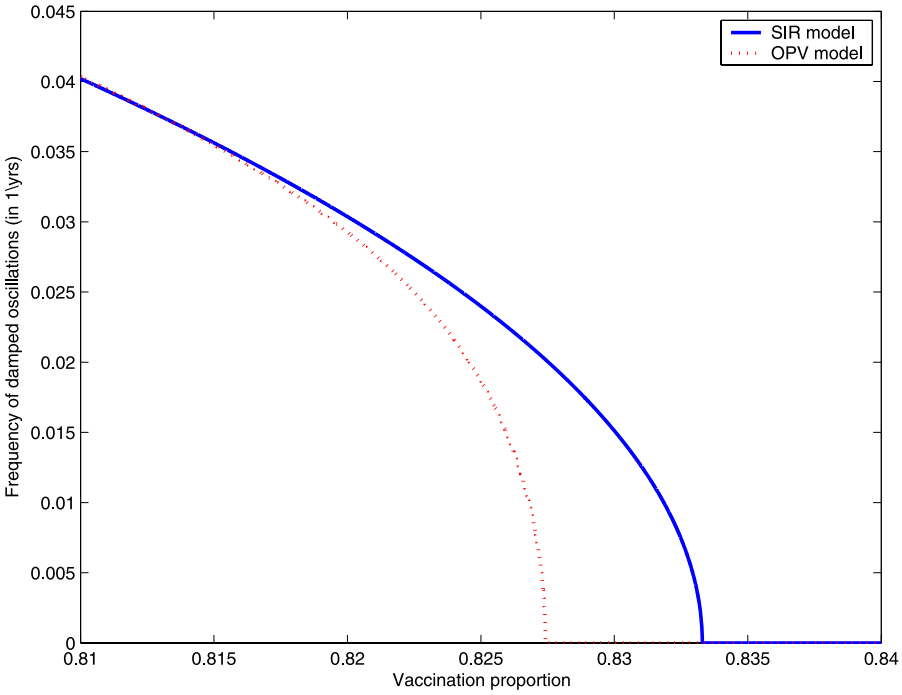

Fig. 2 Frequency of damped oscillations (F_{damp}, (29)) about the globally asymptotically stable endemic equilibrium (17) of the OPV model (11) and the reversion-free SIR polio model, as a function of vaccination proportion (p). The curves are shown only over the narrow range of p for which there is a non-negligible difference in the damping frequencies for the two models. Parameter values, including the estimated OPV reversion proportion (ϕ), are given in Table 1 (the birth rate is that listed for developed countries). Both models exhibit a critical vaccination threshold beyond which the globally stable equilibrium is no longer reached by damped oscillations (p_{crit} in the SIR model). Increasing the value of the reversion proportion ϕ leads to a decrease in this threshold value. For the estimated value of $\phi \simeq 10^{-4}$ (Table 1), this decrease represents only a 0.4% reduction from $p_{\text{crit}} \approx 0.83$ in the reversion-free model. Similar results are obtained if the OPV reversion proportion is taken an order of magnitude higher: $\phi \simeq 10^{-3}$ yields a threshold of $p \simeq 0.81$.

Figure 2 illustrates that for the estimated value of ϕ, the difference in the frequency of damped oscillations compared to zero reversion is negligible. The maximum difference occurs near the SIR model's eradication threshold, $p = p_{\text{crit}}$. As p is increased through p_{crit}, the DFE (6) changes from unstable to globally asymptotically stable. The solid curve in Fig. 2 shows a frequency $F_{\text{damp}} = 0$ for $p \geq p_{\text{crit}}$ because the DFE is not approached by damped oscillations.

While the unique equilibrium of the live-attenuated vaccine model (17) is always endemic (and stable), the manner in which it is approached parallels the distinct behaviors near each of the stable equilibria of the standard SIR model. Figure 2 shows that there is a threshold level of vaccination below which the endemic equilibrium is reached by damped oscillations, and above which there is no oscillatory behavior. This threshold is lower than the SIR model's eradication threshold p_{crit}, though for $\phi = 10^{-4}$ the difference between the thresholds is only 0.4%. Numerical explorations like in Fig. 2 for a wide

range of reversion proportions ($10^{-6} \leq \phi \leq 10^{-2}$) indicate that there is always a threshold value p_{damp} such that damped oscillations occur if and only if $p < p_{\text{damp}}$. Moreover, p_{damp} decreases as ϕ is increased.

4.2.3.2. Rate of convergence To quantify the attractivity of the (globally stable) equilibrium of the OPV model (11), Fig. 3 shows the minimal rate of convergence of solutions in a sufficiently small neighborhood of the equilibrium (17), as a function of the vaccination proportion p. The dashed curve shows the convergence rate for the estimated OPV reversion proportion ϕ (Table 1), while the solid curve shows the convergence rate for the case of no reversion ($\phi = 0$), which corresponds to the standard SIR model. The minimal rate of convergence is calculated as

$$r_{\min} = \min\{-\Re(\lambda_+), -\Re(\lambda_-)\}, \tag{30}$$

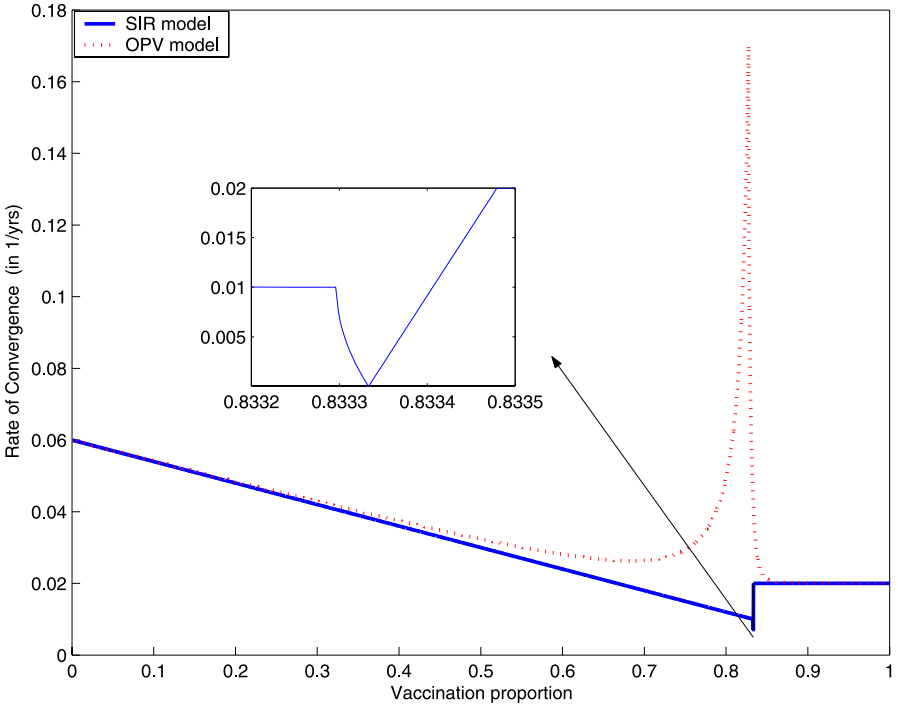

Fig. 3 Local minimum rate of convergence ($r_{\min}$, Eq. (30)) of solutions to the globally asymptotically stable equilibrium for the OPV polio model and the standard SIR polio model without vaccine reversion, as a function of vaccination proportion p. Values of parameters, including the estimated OPV reversion proportion ϕ are given in Table 1. Birth rates used are for developed countries. For high and low levels of vaccination, the local rates of convergence are very similar. However, as the vaccination proportion is increased toward the theoretical vaccination threshold for the SIR polio model, $p_{\text{crit}} \approx 0.83$, the rate for OPV increases sharply to a maximum followed by an equally sharp decrease to rates comparable to those in the SIR polio model. It should be noted that as $p = p_{\text{crit}}$ is a point of stability exchange between the endemic equilibrium and disease free equilibrium in the SIR model, the rate of convergence is zero at this point.

where $\lambda_{\pm}$ are the eigenvalues given in Eq. (19). Note that in the zero reversion case, the convergence rate shown is always to the globally asymptotically stable equilibrium (the endemic equilibrium for $p < p_{\text{crit}}$ and the DFE for $p \geq p_{\text{crit}}$).

Figure 3 shows that for the estimated value of the OPV reversion proportion (Table 1) the rate of convergence onto the globally asymptotically stable equilibrium (17) differs negligibly from the rate for the standard SIR polio model when the vaccination proportion is either significantly greater or significantly smaller than the theoretical SIR eradication threshold p_{crit}. However, when p approaches p_{crit}, the rate of convergence for the OPV model increases sharply, attaining a maximum, and then sharply decreases to the levels of the SIR polio model. In contrast, in the SIR model, as there is an exchange of stability between the endemic and the disease free equilibrium at $p = p_{\text{crit}}$, the rate of convergence is near zero for p in a neighborhood of p_{crit}. When the reversion proportion ϕ is taken orders of magnitude higher or lower, results are qualitatively similar. As ϕ is increased, the maximum value of the rate r_{min} is increased and attained at a lower vaccination proportion p.

4.3. Implications for continuous OPV vaccination

Figure 4 shows, as a function of the vaccination proportion p, the predicted equilibrium number of infectives and annual expected cases of paralytic polio in a (constant) population of one hundred million (i.e., I^*N with I^* from Eq. (17b) and $N = 10^8$). Since the mean time spent in the infected class is $1/(\gamma + \nu)$, and the probability that polio will become paralytic is π_{para} (Table 1), the number of cases of paralytic polio expected in time T as a proportion of the population is

$$P(T) = \pi_{\text{para}} I^*(\gamma + \nu)T. \tag{31}$$

The solid curve in Fig. 4 is based on the parameter estimates in Table 1 (birth rates used are for developed countries), whereas the dotted (dashed) curve uses a value of ϕ that is an order of magnitude below (above) the estimated value. Note that the range of p shown in Fig. 4 is mostly beyond the eradication threshold for the standard SIR ($p_{\text{crit}} \approx 0.83$).

For the estimated value of the reversion factor ($\phi \sim 10^{-4}$), Fig. 4 indicates that even in a population with 90–95% vaccination coverage the model predicts persistence of the disease at an endemic level of 20 to 30 infected individuals per hundred million, and an event rate of two or three cases of paralytic polio per hundred million per year. This prediction agrees closely with the observed event rate in the United States from 1988 to 2000 when OPV was in use (8–10 cases of paralytic polio annually in a population ∼300 million; Anon, 2005a). This agreement suggests that the estimated ϕ is of the right order of magnitude, since the event rate predicted in Fig. 4 is sensitive to ϕ.

The main purpose of the OPV model (11) is to help understand the significance of emergent cVDPVs. This is perhaps best illustrated in Fig. 5, which shows the difference between the endemic number of infectives predicted by the OPV model, Eq. (17b), and the number of infectives predicted by the standard SIR model, Eq. (6) or (10) (the SIR endemic level is also plotted for comparison). For $p \lesssim 0.75$, the difference is negligible (two orders of magnitude smaller than the number of infectives predicted by the standard SIR model). The difference is maximal (∼380 per hundred million population) for $p = 0.83 \approx p_{\text{crit}}$, the eradication threshold in the absence of reversion.

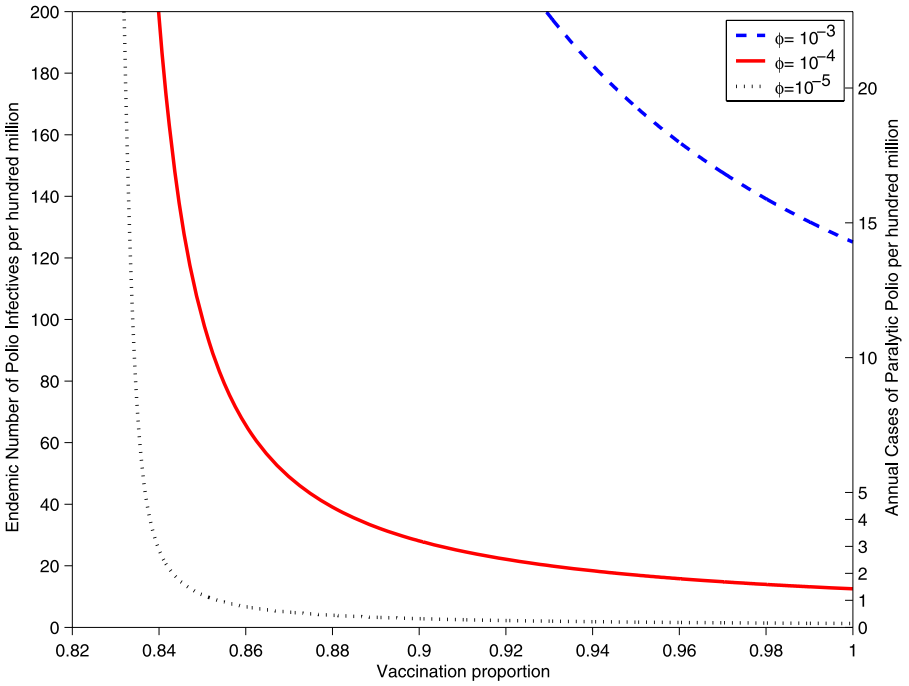

Fig. 4 Equilibrium number of infectives and expected cases of Paralytic Polio annually per hundred million population as a function of OPV vaccination proportion p, for $p > 0.82$. The solid line represents results for the estimated value of the reversion proportion, $\phi \approx 10^{-4}$. A small but significant endemic level of the disease is predicted. Dashed lines represent reversion proportions an order of magnitude above and below the estimated value (10^{-3} and 10^{-5}). Note that for the standard SIR model, eradication of the disease is predicted for all $p > p_{\text{crit}} \approx 0.83$.

We infer that for levels of vaccination even 5% below the theoretical eradication threshold in the absence of reversion (p_{crit}), the impact of cVDPVs is likely to be negligible compared to the impact of the native viruses. Consequently, if coverage levels cannot be brought close to p_{crit} then use of OPV is likely to be easy to justify. However, in situations like the present, where coverage levels reaching p_{crit} are plausibly within reach, it appears that OPV can itself become the primary impediment to eradication.

It should be noted that although Figs. 4 and 5 are plotted using birth rates for developed countries (Table 1), the shape of the curves is practically invariant to the birth rate ν. To see this, note that the equations for the proportion of infected individuals at the endemic equilibrium in the SIR model (6) and the equilibrium in the OPV model (17b) scale linearly with f (8) and are otherwise independent of ν (notwithstanding the negligible dependence of $\mathcal{R}_0$ on ν). Thus Figs. 4 and 5 will scale essentially linearly with birth rates (for birth rates in a realistic range). For example, to produce these figures for birth rates representative of developing countries (Table 1) one need only scale both vertical axes by a factor of 2.

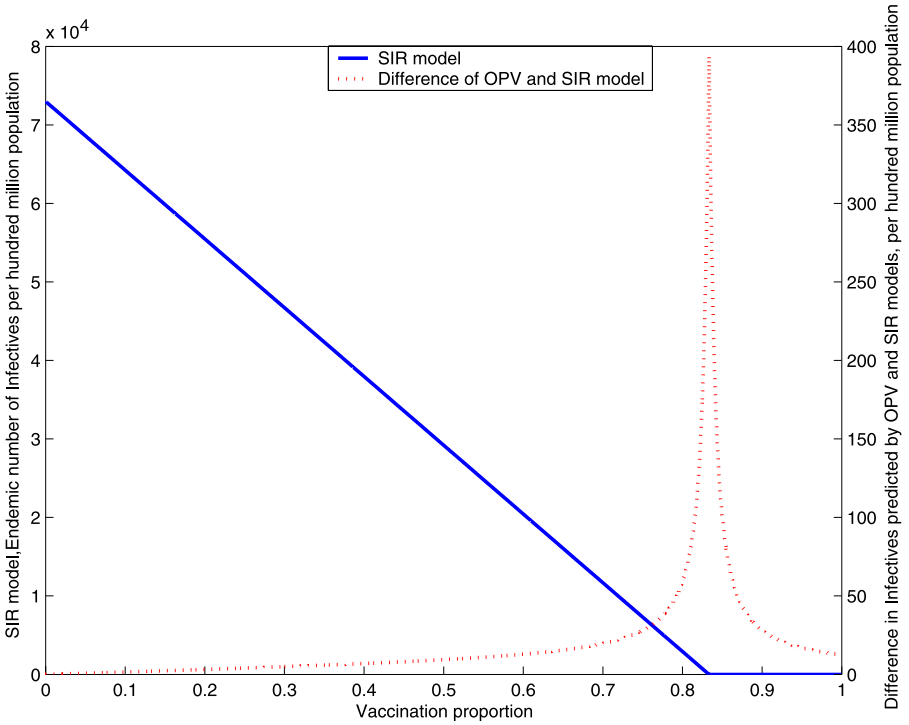

Fig. 5 Effects of reversion on the endemic number of infective individuals at equilibrium. The solid line shows, as a function of vaccination proportion p, the predicted endemic equilibrium for the standard SIR model (4) (which may be thought of as a model of IPV vaccination or a theoretical OPV that never reverts). The dotted curve shows the difference between the predicted endemic number of infectives in the (continuous) OPV vaccination model (17) (with reversion) and the standard SIR model. For vaccination levels even 5% below $p_{\text{crit}} \approx 0.83$, the effect of reversion is negligible. As the vaccination level approaches p_{crit}, the reversion-free SIR model predicts eradication of the disease, while the OPV model with reversion predicts a small but significant endemic level of the disease (note the different scales on the left and right axes of the plot). For the estimated parameters in Table 1, the difference between the models is maximized near p_{crit}, though this is not the case for much larger values of the reversion proportion ϕ.

4.3.1. Sensitivity to distribution of infectious period

In both the SIR model (4) and our OPV reversion model (17), there is an implicit assumption that infectious periods are exponentially distributed. This assumption is usually made in epidemiological modeling because it greatly simplifies the mathematical formulation, yielding a small system of ordinary differential equations. For arbitrary distributions of stage durations, the models become more complex systems of integro-differential Eq. (22).

In general, real distributions of infectious periods are not well-fitted by exponential distributions (Lloyd, 2001). In the context of OPV, there is one potentially advantageous aspect of the exponential distribution: its extremely long tail, i.e., finite probability of individuals remaining infectious for an extremely long time. This may be reasonable for polio because some individuals (with severely compromised immune systems) have been observed to shed poliovirus for extremely long periods (Anon, 2005b). Nevertheless, the

existence of chronic shedders is unlikely to result in a precisely exponential distribution of infectious periods.

Does the implicit assumption of an exponential distribution of infectious periods affect our conclusions? To address this, we examine how the predicted endemic level of infectives (17b) changes as the shape of the infectious period distribution is changed from extremely broad (exponential) to extremely narrow (almost no variation about the mean infectious period, $1/\gamma$).

We suppose the distribution of infectious periods is a Gamma distribution Gamma(n, $\frac{1}{n\gamma}$), with mean $1/\gamma$ and shape parameter n. The probability density for the distribution Gamma(n, $\frac{1}{n\gamma}$) is

$$g\left(x; n, \frac{1}{n\gamma}\right) = \frac{(n\gamma)^n x^{n-1} e^{-n\gamma x}}{\Gamma(n)}, \quad x > 0. \tag{32}$$

For $n = 1$ we obtain the exponential distribution and the limit $n \to \infty$ yields a Dirac delta distribution. The probability densities for several values of n are shown in Fig. 6a.

For integer n, a standard trick (Anderson and Watson, 1980; Bailey, 1964; Lloyd, 2001; Ma and Earn, 2006) allows us to express our OPV model as a system of $n + 1$ ordinary differential equations:

$$\frac{dS}{dt} = (1-p)\nu - \beta I S - \nu S, \tag{33a}$$

$$\frac{dI_1}{dt} = \phi p\nu + \beta I S - (n\gamma + \nu) I_1, \tag{33b}$$

$$\frac{dI_2}{dt} = n\gamma I_1 - (n\gamma + \nu) I_2, \tag{33c}$$

$$\vdots$$

$$\frac{dI_n}{dt} = n\gamma I_{n-1} - (n\gamma + \nu) I_n, \tag{33d}$$

$$\frac{dR}{dt} = (1-\phi) p\nu + n\gamma I_n - \nu R. \tag{33e}$$

Here, the proportion of infectious individuals is $I = \sum_{k=1}^{n} I_k$ and the new infectious subclasses I_k represent a mathematical device with no intended biological interpretation.

In Appendix B, we show that Eq. (33) has a unique endemic equilibrium for any n (not just the case $n = 1$ as considered in previous sections). We computed this endemic equilibrium using the estimated OPV parameters (Table 1), for a large range of shape parameters from $n = 1$ to 1,000. For each n, we verified that the equilibrium is locally stable by numeric computation of the eigenvalues (using the MATLAB function `eig`).

Figure 6b shows the relationship between the equilibrium endemic level of infection (I^*) and the shape parameter (n) for a specific vaccination proportion ($p = 0.85$). For this particular p, it is clear that the effect of distribution shape on I^* is negligible. More generally, for any $p \in [0, 1]$, I^* varies by less than 0.1% if n is varied from 1 to 1000. Thus the predicted endemic level appears to be robust with respect to the distribution of the infectious period.

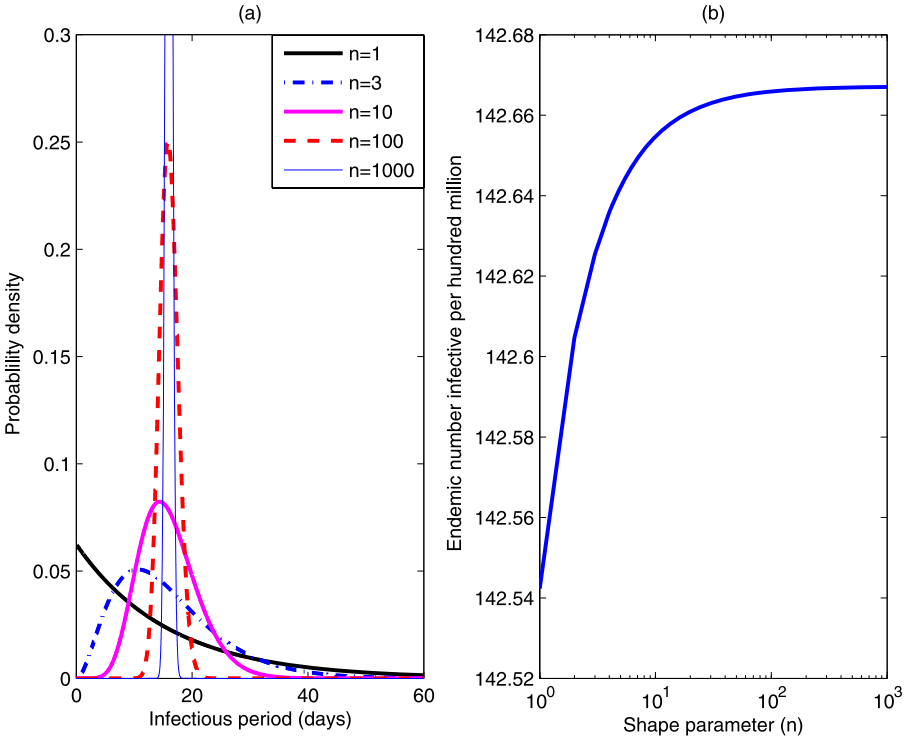

Fig. 6 The effect of the shape of the infectious period distribution on the endemic level of infection in the OPV model (see Section 4.3.1 and Appendix B). (a) Probability density functions for Gamma distributions with mean $\frac{1}{\gamma} = 16$ days and shape parameter n (see Eq. (32)). Note that $n = 1$ yields the exponential distribution. For $n = 1,000$ the peak density value is 0.789. (b) Endemic number of polio infectives per hundred million as a function of distribution shape, for fixed vaccination proportion $p = 0.85$. Epidemiological parameters are as given in Table 1 for developing countries. For fixed mean infectious period, the shape of the full distribution of infectious periods has a negligible effect on the endemic level of polio infection.

5. Final eradication strategies

It is not likely to be possible to eradicate polio using a continuous OPV vaccination strategy, because a continuous source of infectives is inevitable (as a result of reversion). We, therefore, explore the benefits of several alternative polio vaccination strategies that may eliminate the continuous source of new infectious individuals:

(1) Pulsed OPV vaccination. Mass vaccinations are to be performed at regular intervals such as every year or every other year (Agur et al., 1993; Nokes and Swinton, 1997). A revised model incorporating pulsed vaccination is described below.
(2) Switch to continuous IPV vaccination. The standard SIR model is appropriate for IPV because there is no reversion.
(3) One-time mass vaccination with IPV. While continuous IPV vaccination at a high level may not be financially and logistically feasible, given a high level of herd immunity following a broad OPV vaccination program, a single mass IPV campaign

might be sufficient to extinguish the disease. The model required is just a simplification of the pulsed vaccination model (without repeats).

Since genuine eradication means reducing the infective population to zero, the problem can be properly addressed only in a stochastic setting with finite populations. After introducing a model for pulsed vaccination, we turn to stochastic simulations to investigate the above three proposed polio eradication strategies.

5.1. Pulse vaccination models

A pulsed version of our live-attenuated vaccine model (11) can be expressed as the following set of impulsive differential equations.

$$\frac{dS}{dt} = \nu - (\beta I + \nu)S - p\sum_n S(nT^-)\delta(t - nT), \tag{34a}$$

$$\frac{dI}{dt} = \beta IS - (\nu + \gamma)I + \phi p\sum_n S(nT^-)\delta(t - nT), \tag{34b}$$

$$\frac{dR}{dt} = \gamma I + (1 - \phi)p\sum_n S(nT^-)\delta(t - nT) - \nu R, \tag{34c}$$

$$S(nT^-) = \lim_{\epsilon\to 0^+} S(nT - \epsilon), \tag{34d}$$

where the sums are over all integers n. In this pulsed model, vaccinations are performed only at intervals of period T, not continuously. At each pulse time, a proportion p of the susceptible population receives the vaccine. The above equations generalize the pulse vaccination model of Stone and colleagues (Stone et al., 2000) to include the reversion factor ϕ.

If there is only one pulse (at time T), and we consider IPV (no reversion), then the equations simplify to

$$\frac{dS}{dt} = \nu - (\beta I + \nu)S - pS(T^-)\delta(t - T), \tag{35a}$$

$$\frac{dI}{dt} = \beta IS - (\nu + \gamma)I, \tag{35b}$$

$$\frac{dR}{dt} = \gamma I + pS(T^-)\delta(t - T) - \nu R, \tag{35c}$$

$$S(T^-) = \lim_{\epsilon\to 0^+} S(T - \epsilon). \tag{35d}$$

5.2. Stochastic simulations

Equations (4), (34), and (35), represent deterministic models that can be used to explore the three proposed alternative vaccination strategies. However, integrating the differential equations will not allow us to estimate the probability that a given strategy will successfully lead to polio eradication. To that end, we recast these models as continuous time Markov processes, which are fully stochastic and involve finite populations. We use the

standard Gillespie algorithm (Gillespie, 1976), in which the various terms in the differential equations are interpreted as event rates for the various Markov processes involved. (Figure 1 shows all the state transitions that occur, with their rates.)

We are thinking of each of the three proposed strategies as final eradication strategies after a normal, continuous OPV vaccination program has come as close as possible to eradication. Therefore, we take as the initial conditions for our simulations the equilibrium of our model (11) with an assumed OPV coverage level $p = 0.85$ (slightly above the eradication threshold in the absence of reversion, $p_{\text{crit}} \simeq 0.83$). In all simulations, we used a population of one hundred million ($N = 10^8$), and the birth rate was taken to be representative of the developing world (Table 1). The pulsing period was taken to be one year ($T = 1$ yr) and the first pulse was applied immediately after ceasing the continuous OPV program. The one-time IPV vaccination was also applied immediately after ceasing OPV vaccination. The model parameter p in Eq. (34) was varied over the range 0–0.35 while p in Eq. (35) was varied over the range 0–0.40.

5.2.1. Pulsed OPV versus continuous IPV

Figure 7 shows, for the strategies of pulsed OPV and continuous IPV vaccination in a developing region, the probability of polio eradication within 4 years as a function of the effective number of vaccinations performed. Here we define the effective number to be the number of vaccinations performed on susceptible individuals, noting that under a realistic pulse vaccination strategy one might expect the true number of vaccinations to exceed the effective number due to duplicate vaccinations. It should be noted that this definition of effective number has no relationship to reversion. In order to simplify the comparison of the continuous and pulse vaccination strategies, we introduce the idea of the effective vaccination *proportion* for a pulse vaccination strategy, which can be expressed as follows:

$$p_{\text{eff}} = \frac{\overline{V}(T)}{T\nu}, \tag{36}$$

where T is the pulsing period, $\overline{V}(T)$ is the average effective number of vaccinations per pulsing period and ν is the birth rate. Thus, under this definition, a continuous vaccination strategy with vaccination proportion $p = p_{\text{eff}}$ would vaccinate the same number of individuals as the corresponding pulse strategy in a given pulsing period.

Substantial effects of stochasticity are evident in Fig. 7. Even if we cease vaccination altogether (left limit of Fig. 7) there is a non-zero probability that polio will go extinct within 4 years. In developing countries (the situation depicted in Fig. 7), this fadeout probability is very small (less than 1%) but it should be noted that the probability of fadeout after stopping vaccination altogether is much greater for smaller birth rates; in particular, for birth rates typical of developed countries (Table 1), the one-year fadeout probability upon ceasing vaccination is 17%. Sensitivity of fadeout probabilities to birth rates occurs for two reasons: the birth rate determines the rate at which new susceptible individuals are recruited into the population and the equilibrium number of infected individuals is (approximately) proportional to the birth rate (Eq. (17b)).

Continuing to focus on birth rates appropriate for developing countries, we see from Fig. 7 that for any $p_{\text{eff}} < 0.3$ the four-year fadeout probability remains negligible if pulsed

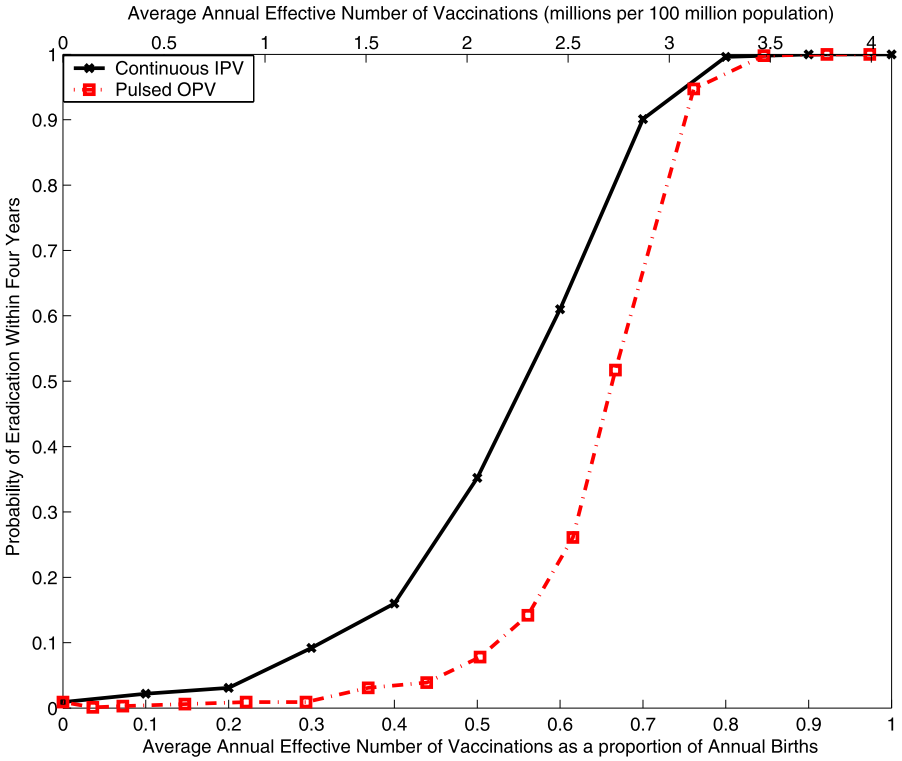

Fig. 7 Probability of Polio eradication within 4 years as a function of the average annual effective number of vaccinations, for annually pulsed OPV (dashed curve) and continuous IPV vaccination (solid curve) in a population of one hundred million (with birth rates typical of developing countries; Table 1). The lower horizontal axis gives the average annual effective number of vaccinations as a proportion of the average annual births as defined by p_{eff} in Eq. (36) (for $T = 1$). For continuous vaccination this reduces to the vaccination proportion p in Eq. (4). The upper horizontal axis gives the raw annual average number of vaccinations (in millions per 100 million population). Continuous IPV campaigns are successful for moderate vaccination coverage ($p \gtrsim 0.7$). For very low vaccination coverage ($p \lesssim 0.3$) pulsed OPV campaigns are no better than ceasing vaccination altogether, due in part to the introduction of infectives through vaccination. However, pulsed OPV can also be successful if a moderate coverage level is achieved ($p_{\text{eff}} > 0.75$), though the vaccination level required is greater than that required for continuous IPV.

OPV is employed, and small ($\sim$10%) if continuous IPV is used. However, moderate vaccination levels ($p_{\text{eff}} \sim 0.7$) yield great improvement. The four-year fadeout probability reaches 90% for $p_{\text{eff}} \sim 0.75$ using OPV or $p_{\text{eff}} \sim 0.7$ with IPV.

In general, pulsed OPV vaccination is less effective than the corresponding IPV strategies with the same number of doses. For small OPV pulses, the probability of eradication is no better than if no OPV vaccination is performed at all (due to the introduction of infectives via reversion). However, for sufficiently large OPV pulses, increased herd immunity outweighs the input of infectives and switching from continuous OPV vaccination to pulsing is likely to be very helpful. In particular, Fig. 7 indicates that switching from 85% continuous OPV vaccination to 85% pulsed OPV vaccination once per year will

change the probability of fadeout within 4 years from zero to nearly 1 using the same number of doses.

5.2.2. Single pulse OPV versus single pulse IPV

The most effective strategy might be the application of one large pulse of IPV, following a successful continuous OPV vaccination campaign. Figure 9 shows the probability of eradication within one year as a function of the effective number of IPV or OPV vaccinations in a one-time pulse. As an example, note from the figure that an application of five million effective doses, representing less than 35% of the susceptible population, leads to a one-year fadeout probability of less than 80% if OPV is used but greater than 95% if IPV is used. Furthermore, as illustrated by Fig. 10, eradication is witnessed in shorter time intervals following IPV vaccination as compared to an equivalent OPV pulse. Thus, a one-time IPV pulse may be desirable both from the perspectives of total number of vaccinations and time to eradication.

5.2.3. Rational policy options

Our models indicate that one-time mass and continuous IPV coverage are effective eradication strategies, even at moderate coverage levels, while pulsed OPV vaccination may be a viable option as long as a sufficiently high level of coverage is maintained. Note that while OPV is much cheaper and easier to administer than IPV, the logistical advantage of needing to reach a much smaller proportion of the population for the same payoff in probability of eradication is an important benefit of IPV.

It should also be noted that in this discussion the IPV model assumes full intestinal immunity of the vaccinated individual. This is, of course, a simplification, and IPV is generally thought to induce lower levels of intestinal immunity compared to OPV (Laasri et al., 2005). Consequently, it is likely that the eradication probabilities that we have predicted for the IPV programs are overestimated (by an unknown amount). The significance of lowered gut immunity is still an open question, though as previously mentioned, recent studies suggest that enhanced potency IPV (eIPV) induces an improved level of intestinal immunity over previous IPV offerings (Laasri et al., 2005).

6. Summary and conclusions

We have presented a compartmental model that takes into account the possibility of reversion in live attenuated virus vaccines (Fig. 1 and Eqs. (11)). For a non-zero reversion proportion of the vaccine ($\phi > 0$), the model has one biologically meaningful (endemic) equilibrium, which is globally asymptotically stable.

We applied the model to polio dynamics, assuming oral polio vaccine (OPV) is given to a fixed proportion of newborns (p), and investigated the impact of circulating vaccine derived polio viruses (cVDPVs). For our estimated value of the reversion proportion ($\phi \sim 10^{-4}$; Table 1), we found that for vaccination levels (p) less than 75% the effect of cVDPVs is negligible compared to the expected endemic level of the disease in the absence of reversion. We concluded that if OPV coverage levels are below the critical level required for eradication in the absence of reversion ($p < p_{\text{crit}} \simeq 0.83$), then it is best to focus on trying to increase OPV coverage levels (the benefits of increased coverage far outweigh the negative impact of vaccine reversion). However, if p can be brought close

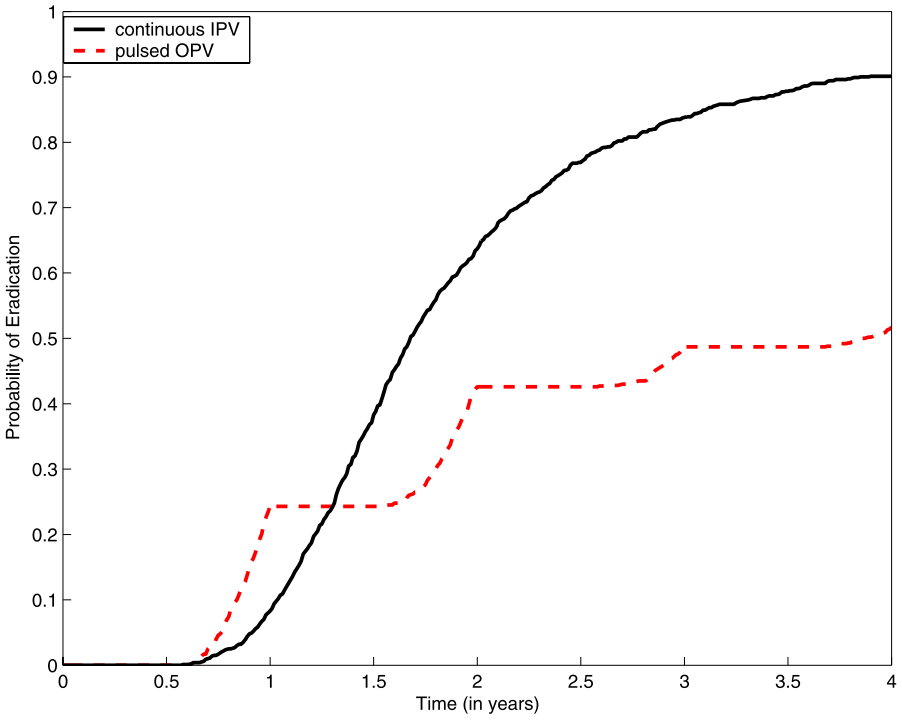

Fig. 8 Probability of Polio eradication as a function of time for a 4 year continuous IPV vaccination program with vaccination proportion $p = 0.7$ (solid curve) and pulse OPV with vaccination parameter $p = 0.2$ and pulse period $T = 1$ yr, corresponding to $p_{\text{eff}} \simeq 0.7$ (see Eq. (36)). The population size is one hundred million with birth rates typical of developing countries (Table 1). Non-zero probability of eradication is apparent slightly after half a year for both strategies. For OPV pulses, there is little increase in eradication probability for roughly half a year following each pulse, due to the pulse introducing a significant number of infectives via vaccine reversion. It should be noted that both strategies exhibit quickly diminishing returns, with the bulk of eradications occurring within the first 2 years of simulations.

to p_{crit} then other strategies should be considered to increase the probability of eradication (the inevitable input of new cVDPVs resulting from continuous OPV vaccination must be avoided).

We considered three alternative eradication strategies that eliminate continuous input of cVDPVs: pulsed OPV vaccination, continuous injectable polio vaccine (IPV) vaccination, and one-time mass IPV vaccination. Based on simulations of stochastic models, we found that continuous or mass IPV vaccination achieves a higher probability of eradication (per dose) than pulsed OPV. In spite of the much greater cost per dose for IPV, we expect that investment in IPV vaccination following a successful continuous OPV campaign will be more effective because the time to eradication is likely to be substantially shorter (Figs. 8 and 10).

The key parameter in our models is the reversion factor ϕ, which can be estimated only crudely. Our modeling would benefit from a more precise estimate of ϕ, noting that by reversion we mean regaining both virulence and transmissibility. Revertant vaccine viruses

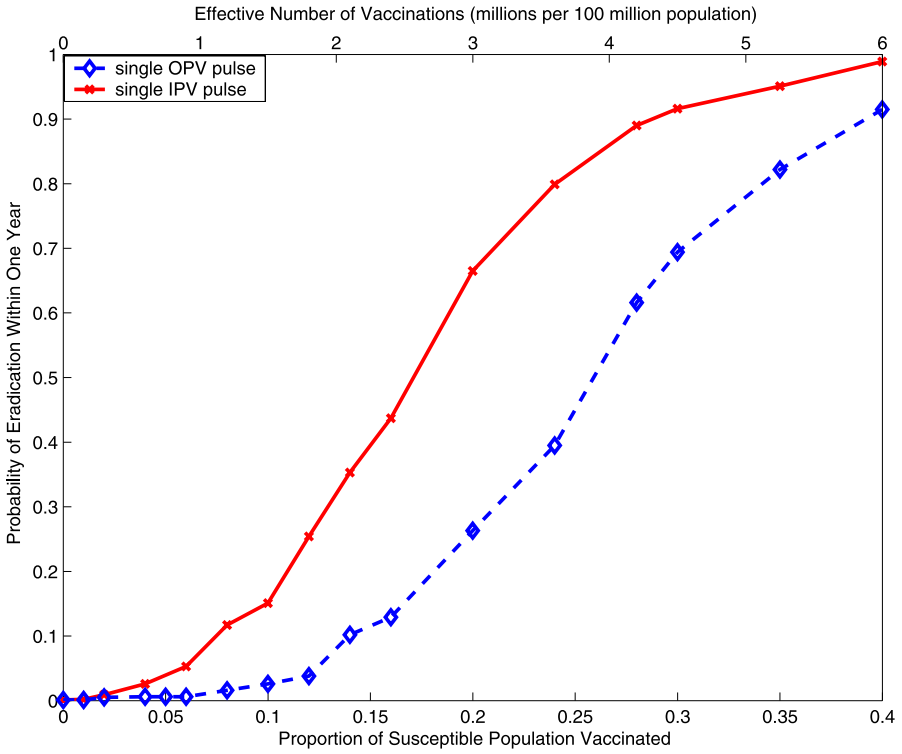

Fig. 9 Probability of Polio eradication within one year, as a function of the effective number of vaccinations for a single vaccine pulse of IPV or OPV in a population of one hundred million (with birth rates typical of developing countries; Table 1). The lower horizontal axis shows the proportion of susceptibles vaccinated (parameter p in Eq. (35); note that $\phi = 0$ for IPV as there is no reversion). The upper horizontal axis shows the total number of vaccinations given. IPV achieves superior eradication probabilities in comparison to OPV for equivalent numbers of vaccinations. Note that for less than five million IPV vaccinations, corresponding to less than 35% of the susceptible population (as given by Eq. (17a)), the probability of eradication within one year is 95%.

probably do not always regain full transmissibility, so an estimate of $\mathcal{R}_0$ for revertant strains would be helpful.

We have ignored the benefit of contact vaccination via OPV: because the vaccine is live, vaccinated individuals can transmit the vaccine and thereby immunize non-vaccinated individuals. This effect should (slightly) lower the predicted endemic number of infectives below that predicted by our model.

With respect to final eradication strategies, a more thorough understanding of IPV's effectiveness in inducing gut immunity is needed. In addition, polio models accounting for spatial heterogeneity and seasonality in transmission rates should be investigated, since synchronization of fadeouts could increase the probability of eradication (Earn et al., 1998, 2000; Earn and Levin, 2006).

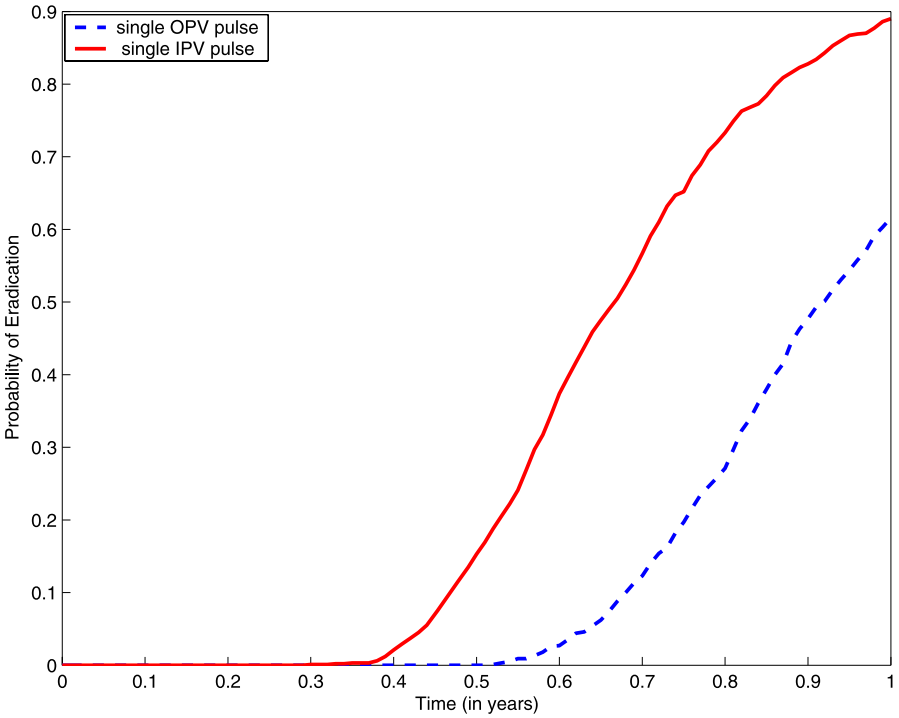

Fig. 10 Probability of polio eradication as a function of time, for a single vaccine pulse of IPV ($\phi = 0$) or OPV (ϕ as in Table 1) with $p = 0.28$ (where p is the susceptible vaccination proportion in Eq. (35)). The population is one hundred million (with birth rates typical of developing countries; Table 1). For IPV, non-zero probability of eradication is apparent for shorter time intervals in comparison to OPV. Non-zero probability of eradication for OPV is observed almost 2 months later than for IPV.

Appendix A:

We show here that if $0 < p < 1$ and $0 < \phi \leq 1$ then the equilibrium given by (17) is contained in the biologically relevant region $\mathcal{B} = \{(S, I) : S > 0, I > 0, S + I < 1\}$.

First, if $p\phi > 0$ then

$$\sqrt{\left[\frac{1}{2}\Delta p\right]^2 + \frac{p\phi}{\mathcal{R}_0}} > \left|\frac{1}{2}\Delta p\right|, \tag{A.1}$$

so $I^* > 0$ in Eq. (17b).

Second, we can re-express Eq. (17a) as

$$S^* = 1 - p_{\text{crit}} + \frac{1}{2}\Delta p - \sqrt{\left[\frac{1}{2}\Delta p\right]^2 + \frac{p\phi}{\mathcal{R}_0}}. \tag{A.2}$$

Since $1 - p_{\text{crit}} = 1/\mathcal{R}_0$, we therefore have

$$S^* > 0 \iff \frac{1}{\mathcal{R}_0} + \frac{1}{2}\Delta p > \sqrt{\left[\frac{1}{2}\Delta p\right]^2 + \frac{p\phi}{\mathcal{R}_0}}, \tag{A.3a}$$

$$\iff \left(\frac{1}{\mathcal{R}_0} + \frac{1}{2}\Delta p\right)^2 > \left[\frac{1}{2}\Delta p\right]^2 + \frac{p\phi}{\mathcal{R}_0}, \tag{A.3b}$$

$$\iff \frac{1}{\mathcal{R}_0^2} + \frac{\Delta p}{\mathcal{R}_0} > \frac{p\phi}{\mathcal{R}_0}, \tag{A.3c}$$

$$\iff \frac{1}{\mathcal{R}_0} + \left(1 - \frac{1}{\mathcal{R}_0}\right) - p(1-\phi) > p\phi, \tag{A.3d}$$

$$\iff p < 1. \tag{A.3e}$$

Finally, summing Eqs. (17a) and (17b) to obtain

$$S^* + I^* = \frac{1}{\mathcal{R}_0} + \frac{1}{2}(1+f)\Delta p - (1-f)\sqrt{\left[\frac{1}{2}\Delta p\right]^2 + \frac{p\phi}{\mathcal{R}_0}}, \tag{A.4}$$

and defining

$$F(f) = 1 - (S^* + I^*), \tag{A.5}$$

we must show $F(f) > 0$ for all relevant values of f (i.e., for $0 < f < 1$ from definition (8)). To see this, note that

$$F(1) = 1 - \frac{1}{\mathcal{R}_0} - \Delta p = p(1-\phi) \geq 0 \tag{A.6}$$

and

$$\frac{dF}{df} = -\frac{1}{2}\Delta p - \sqrt{\left[\frac{1}{2}\Delta p\right]^2 + \frac{p\phi}{\mathcal{R}_0}} \tag{A.7a}$$

$$< 0 \quad \text{for all } f, \tag{A.7b}$$

so $F(f) > 0$ for all $f < 1$.

Appendix B:

We formally calculate the endemic equilibrium of the Gamma distributed OPV reversion model (33). We use the superscript * to denote the equilibrium value and we define the dimensionless parameter

$$f_n = \frac{\nu}{n\gamma + \nu}. \tag{B.1}$$

For $n = 1$, f_n reduces to f, as defined in Eq. (8). For the Gamma distributed SIR model, the *basic reproductive number* $\mathcal{R}_0$ is given by van den Driessche and Watmough (2002)

$$\mathcal{R}_0 = \frac{\beta}{\nu}\big(1 - (1 - f_n)^n\big). \tag{B.2}$$

In terms of $\mathcal{R}_0$, the *critical vaccination proportion* (which is meaningful in the absence of reversion) is still given by the usual formula (9).

Setting Eq. (33) to zero, for $k \geq 2$ we find

$$I_k^* = (1 - f_n) I_{k-1}^* \tag{B.3}$$

and hence

$$I_k^* = (1 - f_n)^{k-1} I_1^*. \tag{B.4}$$

We therefore have

$$I^* = \sum_{k=1}^{n} I_k^* = \frac{1 - (1 - f_n)^n}{1 - (1 - f_n)} I_1^* = \frac{1 - (1 - f_n)^n}{f_n} I_1^*. \tag{B.5}$$

Summing Eqs. (33a) and (33b) at equilibrium yields

$$S^* = 1 - p(1 - \phi) - \frac{1}{f_n} I_1^*. \tag{B.6}$$

Substituting Eq. (B.6) into (33b) (set to zero), expressing I^* in terms of I_1^* via (B.5) and simplifying in terms $\mathcal{R}_0$ yields the quadratic equation

$$\frac{1}{f_n} I_1^{*2} - \big[p_{\text{crit}} - p(1 - \phi)\big] I_1^* - \frac{p\phi f_n}{\mathcal{R}_0} = 0. \tag{B.7}$$

This quadratic equation for I_1^* has exactly the same form as Eq. (14) for I^* in the case $n = 1$. As in Section 4.1, defining $\Delta p = p_{\text{crit}} - p(1 - \phi)$ and solving the quadratic for I_1^* (insisting that it be non-negative) yields the unique solution

$$I_1^* = f_n \left[\frac{1}{2}\Delta p + \sqrt{\left[\frac{1}{2}\Delta p\right]^2 + \frac{p\phi}{\mathcal{R}_0}} \right] \tag{B.8}$$

from which Eqs. (B.5) and (B.6) imply

$$I^* = \big[1 - (1 - f_n)^n\big] \left[\frac{1}{2}\Delta p + \sqrt{\left[\frac{1}{2}\Delta p\right]^2 + \frac{p\phi}{\mathcal{R}_0}} \right], \tag{B.9a}$$

$$S^* = 1 - p(1 - \phi) - \frac{1}{2}\Delta p - \sqrt{\left[\frac{1}{2}\Delta p\right]^2 + \frac{p\phi}{\mathcal{R}_0}}. \tag{B.9b}$$

As expected, for the exponential distribution ($n = 1$), Eq. (B.9) reduces to (17).

Appendix C:

Here we show that for the live attenuated virus model (11), if $0 < p < 1$ and $0 < \phi < 1$ then the region $\mathcal{B} = \{(S, I) : S > 0, I > 0, S + I < 1\}$ is forward invariant, and for all initial conditions along the boundary of $\mathcal{B}$ the flow of Eq. (11) is into $\mathcal{B}$.

As shown in Section 3, since the model (11) is constructed in terms of proportions, the closure of $\mathcal{B}$ is forward invariant. Therefore, it is sufficient to show that the flow of (11) along the boundary of $\mathcal{B}$ is into $\mathcal{B}$.

The boundary is given by the lines $S = 0$, $I = 0$ and $S + I = 1$. Along the line $S = 0$, the flow of (11) is given by

$$\left.\frac{dS}{dt}\right|_{S=0} = (1 - p)\nu, \tag{C.1}$$

which is positive for any $p < 1$. Hence the flow along the line $S = 0$ is into $\mathcal{B}$. Similarly, if $I = 0$ then

$$\left.\frac{dI}{dt}\right|_{I=0} = \phi p\nu, \tag{C.2}$$

which is positive provided $p > 0$ and $\phi > 0$. Finally, along the line $S + I = 1$,

$$\left.\frac{d(S+I)}{dt}\right|_{S+I=1} = -(1-\phi)p\nu - \gamma I \leq -(1-\phi)p\nu, \tag{C.3}$$

which is negative provided $\phi < 1$ and $p > 0$. Thus, the flow along the boundary lines is into $\mathcal{B}$.

References

Agur, Z., Cojocaru, L., Mazor, G., Anderson, R.M., Danon, Y.L., 1993. Pulse mass measles vaccination across age cohorts. Proc. Natl. Acad. Sci. USA 90, 11698–11702.

Anderson, R.M., May, R.M., 1991. Infectious Diseases of Humans, Dynamics and Control. Oxford Science Publications.

Anderson, D., Watson, R., 1980. On the spread of a disease with gamma distributed latent and infectious periods. Biometrika 67(1), 191–198.

Anon, 1994. Polio Eradication Field Guide Technical Paper No. 40. Technical Report, Word Health Organization and Pan American Health Organization.

Anon, 2001. National Vital Statistics Report. Technical Report 49 (1), National Center for Health Statistics, http://www.cdc.gov/nchs/data/natality/nvs49_1t1.pdf.

Anon, 2005a. Diseases and Conditions: Polio. Technical Report, Centers for Disease Control and Prevention, http://www.cdc.gov/nip/publications/pink/polio.pdf.

Anon, 2005b. Morb. Mortal Wkly Rep. Technical Report 41, CDC.

Bailey, N., 1964. Some stochastic models for small epidemics in large populations. Appl. Stat. 13(1), 9–19.

Brauer, F., 2003. Backward bifurcations in simple vaccination models. J. Math. Anal. Appl. 298, 418–431.

Earn, D.J.D., Levin, S.A., 2006. Global asymptotic coherence in discrete dynamical systems. Proc. Natl. Acad. Sci. USA 103(11), 3968–3971.

Earn, D.J.D., Rohani, P., Grenfell, B.T., 1998. Persistence chaos and synchrony in ecology and epidemiology. Proc. Roy. Soc. Lond. Ser. B Biol. Sci. 265(1390), 7–10.

Earn, D.J.D., Levin, S.A., Rohani, P., 2000. Coherence and conservation. Science 290(5495), 1360–1364.

Gillespie, D.T., 1976. A general method for numerically simulating the stochastic time evolution of coupled chemical reactions. J. Comput. Phys. 22, 403–434.
Grassly, N.C., Wenger, J., Durrani, S., Bahl, S., Deshpande, J.M., Sutter, R.W., Heymann, D.L., Aylward, R., 2007. Protective efficacy of a monovalent oral type 1 poliovirus vaccine: a case-control study. Lancet 369, 1356–1362.
Hethcote, H.W., 2000. The mathematics of infectious diseases. SIAM Rev. 42(4), 599–653.
Heymann, D.L., Sutter, R.W., Aylward, R.B., 2005. A global call for new polio vaccines. Nature 434, 699–700.
John, J., 2004. A developing country perspective of vaccine associated paralytic poliomyelitis. Bull. World Health Organ. 82, 53–58.
Kermack, W.O., McKendrick, A.G., 1927. A contribution to the mathematical theory of epidemics. Proc. Roy. Soc. Lond. Ser. A 115, 700–721.
Korobeinikov, A., Wake, G.C., 2002. Lyapunov functions and global stability for SIR, SIRS, and SIS epidemiological models. Appl. Math. Lett. 15, 955–960.
Laasri, M., Lottenbach, K., Belshe, R., Wolff, M., Rennels, M., Plotkin, S., Chumakov, K., 2005. Effect of different vaccination schedules on excretion of oral poliovirus vaccine strains. J. Infect. Dis. 193, 2092–2098.
Lloyd, A.L., 2001. Realistic distributions of infectious periods in epidemic models: changing patterns of persistence and dynamics. Theor. Popul. Biol. 60, 59–71.
Ma, J., Earn, D.J.D., 2006. Generality of the final size formula for an epidemic of a newly invading infectious disease. Bull. Math. Biol. 68, 679–702.
McDevitt, T., 1999. World Population Profile: 1998. Technical Report, U.S. Census Bureau, http://iggi.unesco.or.kr/web/iggi_docs/05/952662740.pdf.
Nokes, D.J., Swinton, J., 1997. Vaccination in pulses: a strategy for global eradication of measles and polio? Trends Microbiol. 5(1), 14–19.
Offit, P.A., 2005. The Cutter Incident. Yale University Press, New Haven.
Perko, L., 1996. Differential Equations and Dynamical Systems. Springer, Berlin.
Stone, L., Shulgin, B., Agur, Z., 2000. Theoretical examination of the pulse vaccination policy in the SIR epidemic model. J. Math. Comput. Model. 31, 207–215.
van den Driessche, P., Watmough, J., 2002. Reproduction numbers and sub-threshold endemic equilibria for compartmental models of disease transmission. Math. Biosci. 180, 29–48.
Woodrow, G.C., Levine, M.M., 1990. New Generation Virus Vaccines. Dekker, New York.